Photon density wave for imaging through random media

Sermsak Jaruwatanadilok, Akira Ishimaru and Yasuo Kuga

Department of Electrical Engineering, PO Box 352500, University of Washington, Seattle,
WA 98195, USA

E-mail: sermsak@ee.washington.edu

Abstract
The passage of a photon density wave through random media has
been investigated extensively for medical imaging based on the diffusion
approximation. In this paper, the photon density wave is studied based on
the exact time-dependent vector radiative transfer theory. Both continuous and
pulse photon density waves are analysed in a plane parallel medium using Mie
scattering and the discrete ordinates method. The photon density wave shows
superior properties over regular waves in several aspects. It has a narrower
angular spectrum and maintains the original pulse shape. It also preserves
the degree of polarization and increases the cross-polarization discrimination.
These properties of a photon density wave suggest its potential for improving
imaging. Thus, we apply the photon density wave to an imaging problem and
show that it improves the quality of the images compared to other conventional
imaging techniques.

(Some figures in this article are in colour only in the electronic version)

1. Introduction

Many studies on the behaviour of photon density waves in random media have been reported
in recent years [1–9]. Photon density waves make use of modulated intensities with the
modulation frequency typically in the radio wave range. An example of a pulse photon density
wave is visualized in figure 1. The modulated intensity propagates through the scattering
medium and exhibits amplitude and phase variations. However, unlike the wave field which
satisfies the wave equation, the photon density wave satisfies the frequency-dependent radiative
transfer equation. It is similar to the temperature field, which can also behave as a wave, and
the electromagnetic field in a highly conducting medium.

Photon density waves have been utilized in medical optics for optical imaging in
a biological medium. Even though it has been extensively studied using the diffusion
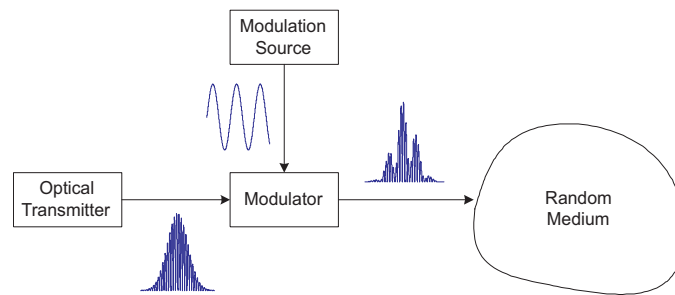
Figure 1. Pulse photon density wave.

approximation, the exact solution should be based on the time-dependent radiative transfer theory. It should be noted that the diffusion approximation is useful for many problems of complex geometries, while the radiative transfer equation has been solved for a limited number of simple geometries. One such problem is the transmission and reflection of a plane wave incident upon a plane-parallel scattering medium.

In this paper, we consider the time-dependent Stokes vector representation of a photon density wave propagating through a slab of discrete random medium in a plane parallel geometry. The discrete random medium is defined as small discrete dielectric spheres suspended in a homogenous background. Examples of such media are fog particles in the air and biological tissues. Using the calculated results based on the time-dependent vector radiative transfer equation, we investigate several properties of the photon density wave. These important properties are the angular spectrum (intensity as a function of angle), the degree of polarization (DOP) and cross-polarization discrimination (XPD). Our previous works [10–13] explain the solution of the pulse vector radiative transfer equation using the discrete ordinates method. With some modification, we are able to adapt the previous method to solve for the solution of the photon density wave with a similar procedure.

Furthermore, we study the formation of the images through the random media and apply several techniques to improve the quality of the images. From the knowledge acquired using the solutions of the radiative transfer equation, we study several techniques to improve the quality of the images. They are off-axis intensity subtraction (OAIS) and cross-polarization intensity subtraction (CPIS) explained in our previous study [14]. These methods are based on reducing the incoherent intensity caused by the scattering. They are compared with the photon density wave imaging. We consider the imaging properties of the focusing system for the incident plane wave with linear and circular polarizations. The term *contrast* is introduced to quantitatively measure the image quality. A detailed analysis of how the images are formed is discussed in [15].

This paper is organized as follows: in section 2, we summarize the basic idea and the governing time-dependent vector radiative transfer equation for photon density waves in random media. We explain the procedure of solving the equation using the discrete ordinates method. Linearly and circularly polarized photon density waves through a random medium are calculated. The results are the Stokes parameters representing the intensity and the polarization state. Then, the time and angular behaviours of those Stokes parameters are explained in section 3. Next, we investigate the application of the photon density wave to imaging in section 4. We compare the cross images using the conventional co-polarized component, off-axis subtraction technique and cross-polarized subtraction technique with the images using the photon density wave. Finally, our conclusions are presented in section 5.
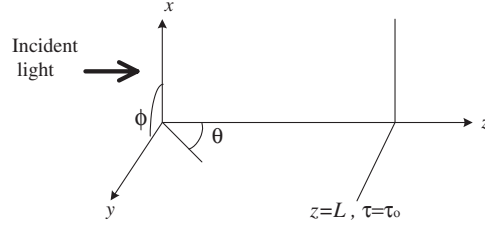
Figure 2. The plane-parallel problem.

2. The photon density radiative transfer equation and its solutions

We consider a plane wave propagating through a slab of random medium of thickness L in a plane-parallel geometry as shown in figure 2. Here, the random media is defined as randomly located dielectric spheres suspended in a homogeneous background. We study the modified Stokes vector which explains the intensity and the polarization state of the wave. The equation that explains the modified Stoke parameters through this random medium in both time and space domains is the narrow-band, time-dependent vector radiative transfer equation expressed as

$$\left(\mu\frac{\partial}{\partial z} + \rho\sigma_t + \frac{1}{c}\frac{\partial}{\partial t}\right)\boldsymbol{I}(t, z, \mu, \phi) = \int_0^{2\pi}\int_{-1}^1 \boldsymbol{S}(\mu, \phi, \mu', \phi')\boldsymbol{I}(t, z, \mu', \phi')\,\mathrm{d}\mu'\,\mathrm{d}\phi'$$
$$+ \boldsymbol{J}(t, z, \mu, \phi), \qquad \text{for } 0 \leqslant z \leqslant L \tag{1}$$

where $\mu = \cos\theta$, ρ is the number density, σ_t is the total scattering of a single particle and c is the speed of the wave in the medium. The modified Stokes vector $\boldsymbol{I}$ is defined by

$$\boldsymbol{I} = [I_1 \quad I_2 \quad U \quad V]^T \tag{2}$$

where T denotes the transpose operator of a matrix. The Mueller matrix $\boldsymbol{S}$ is explained in [13]. It characterizes the scattering behaviour of the random media. The source term is denoted by $\boldsymbol{J}$.

To make the equation easier to handle, we normalize the space domain with $\rho\sigma_t$ and the time domain with L/c. Thus, equation (1) becomes

$$\left(\mu\frac{\partial}{\partial\tau} + 1 + \frac{1}{\tau_0}\frac{\partial}{\partial t_n}\right)\boldsymbol{I}(t_n, \tau, \mu, \phi) = \int_0^{2\pi}\int_{-1}^1 \boldsymbol{S}(\mu, \phi, \mu', \phi')\boldsymbol{I}(t_n, \tau, \mu', \phi')\,\mathrm{d}\mu'\,\mathrm{d}\phi'$$
$$+ \boldsymbol{J}(t_n, \tau, \mu, \phi), \qquad \text{for } 0 \leqslant \tau \leqslant \tau_0 \tag{3}$$

where $\tau = \rho\sigma_t z$ is the *optical distance*, $\tau_o = \rho\sigma_t L$ is the *optical depth* and $t_n = t(L/c)^{-1}$ is the normalized time. For convenience, we omit the subscript n and denote t as the normalized time. To make the total intensity a positive quantity, the photon density wave consists of the constant term and the time-dependent term, i.e.

$$\boldsymbol{I}_{total}(t) = \boldsymbol{I}_{constant} + \boldsymbol{I}(t)\exp(-\mathrm{i}\omega_{mod}t) \tag{4}$$

where $\omega_{mod} = 2\pi f_{mod}$ and f_{mod} is the modulation frequency. We only consider the time-dependent term in our development.

For ease of calculations, the modified Stokes vector is often divided into two parts: the reduced intensity (coherent) modified Stokes vector and the diffuse (incoherent) modified Stokes vector. The reduced intensity modified Stokes vector is the component that decreases due to the scattering and absorption from the particles. It satisfies the equation

$$\frac{\partial}{\partial\tau}\boldsymbol{I}_{ri} = -\boldsymbol{I}_{ri} \tag{5}$$

where I_{ri} denotes the reduced intensity modified Stokes vector. In the plane wave case, it is expressed as

$$I_{ri}(t, \tau) = I_0 f(t, \tau) \exp(-\tau) \delta(\phi) \delta(\mu - 1). \tag{6}$$

I_0 is the incident modified Stokes vector. We consider two cases of incident waves. For linear polarization in the x direction, the incident modified Stokes vector is

$$I_0 = [1 \quad 0 \quad 0 \quad 0]^T \tag{7}$$

and for left-handed circular polarization, it is

$$I_0 = [1/2 \quad 1/2 \quad 0 \quad 1]^T. \tag{8}$$

The pulse shape function for the photon density waves $f(t, \tau)$ is defined as

$$f(t, \tau) = \begin{cases} \exp\left[-i\omega_m\left(t - \dfrac{\tau}{\tau_0}\right)\right] & \text{for continuous wave} \\[2mm] \delta\left(t - \dfrac{\tau}{\tau_0}\right) \exp\left[-i\omega_m\left(t - \dfrac{\tau}{\tau_0}\right)\right] & \text{for delta function pulse} \\[2mm] \dfrac{1}{\sqrt{\pi}\, T_0} \exp\left[-\dfrac{(t - \tau/\tau_0)^2}{T_0^2} - i\omega_m\left(t - \dfrac{\tau}{\tau_0}\right)\right] & \text{for Gaussian pulse} \end{cases} \tag{9}$$

where $\omega_m = \omega_{mod}(L/c)$ is the normalized angular modulation frequency and T_0 is the pulse width in the Gaussian pulse wave case. The regular wave case is easily realized by letting $\omega_m = 0$.

Another component, the diffuse modified Stokes vector I_d, satisfies the equation

$$\left(\mu \frac{\partial}{\partial \tau} + 1 + \frac{1}{\tau_0} \frac{\partial}{\partial t}\right) I_d(t, \tau, \mu, \phi) = \int_0^{2\pi} \int_{-1}^1 S(\mu, \phi, \mu', \phi') I_d(t, \tau, \mu', \phi') \, d\mu' \, d\phi'$$
$$+ E_{ri}(t, \tau, \mu, \phi), \qquad \text{for } 0 \leqslant \tau \leqslant \tau_0. \tag{10}$$

In our calculations, we assume a source-free medium. Thus, the source term J only has the contribution from the incident wave. It is defined as the equivalent source term E_{ri}, given by

$$E_{ri} = \int_0^{2\pi} \int_{-1}^1 S(\mu, \phi, \mu', \phi') I_{ri}(t, \tau, \mu', \phi') \, d\mu' \, d\phi'$$
$$= F_0(\mu, \phi) f(t, \tau) \exp(-\tau) \tag{11}$$

where $F_0(\mu, \phi) = S(\mu, \phi 1, 0) I_0$.

To be able to solve equation (10), we use the Fourier transform to obtain the frequency-domain vector radiative transfer equation expressed as

$$\left(\mu \frac{\partial}{\partial \tau} + 1 - i\frac{\omega}{\tau_0}\right) I_d(\omega, \tau, \mu, \phi) = \int_0^{2\pi} \int_{-1}^1 S(\mu, \phi, \mu', \phi') I_d(\omega, \tau, \mu', \phi') \, d\mu' \, d\phi'$$
$$+ F_0(\mu, \phi) f(\omega, \tau) \exp(-\tau), \qquad \text{for } 0 \leqslant \tau \leqslant \tau_0 \tag{12}$$

where

$$I_d(\omega, \tau, \mu, \phi) = \int I_d(t, \tau, \mu, \phi) \exp(i\omega t) \, dt. \tag{13}$$

ω is the normalized angular frequency, and the pulse shape function in the frequency domain is given by

$$f(\omega, \tau) = \int f(t, \tau) \exp(i\omega t) \, dt. \tag{14}$$

Then, the pulse shape function in equation (9) becomes

$$
f(\omega, \tau) = \begin{cases} \exp\left(-\mathrm{i}\omega\dfrac{\tau}{\tau_0}\right) 2\pi\delta(\omega - \omega_m) & \text{for continuous wave} \\[3mm] \exp\left(-\mathrm{i}\omega\dfrac{\tau}{\tau_0}\right) & \text{for delta function pulse} \\[3mm] \exp\left(-\mathrm{i}\omega\dfrac{\tau}{\tau_0}\right) \exp\left[-\dfrac{(\omega - \omega_m)^2 T_0^2}{4}\right] & \text{for Gaussian pulse.} \end{cases} \quad (15)
$$

Let $\omega = \omega_m + \omega'$ and $\boldsymbol{I}_d'(\omega, \tau) = \boldsymbol{I}_d(\omega, \tau)\exp(-\mathrm{i}\omega\tau/\tau_0)$, equation (12) becomes

$$
\left[\mu\frac{\partial}{\partial\tau} + 1 + (\mu - 1)\mathrm{i}\frac{\omega' + \omega_m}{\tau_0}\right] \boldsymbol{I}_d'(\omega', \tau, \mu, \phi)
$$
$$
= \int_0^{2\pi}\int_{-1}^1 \boldsymbol{S}(\mu, \phi, \mu', \phi')\boldsymbol{I}_d'(\omega', \tau, \mu', \phi')\,\mathrm{d}\mu'\,\mathrm{d}\phi'
$$
$$
+ \boldsymbol{F}_0(\mu, \phi)f(\omega', \tau)\exp(-\tau), \qquad \text{for } 0 \leqslant \tau \leqslant \tau_0 \quad (16)
$$

where

$$
f(\omega', \tau) = \begin{cases} 2\pi\delta(\omega') & \text{for continuous wave} \\[2mm] 1 & \text{for delta function pulse} \\[2mm] \exp\left(-\dfrac{\omega'^2 T_0^2}{4}\right) & \text{for Gaussian pulse.} \end{cases} \quad (17)
$$

Equation (16) is in a much simpler form to solve. It also eliminates the instability caused by the high-frequency component in the function $f(\omega, \tau)$. We solve this equation by imposing the boundary conditions given by

$$
\boldsymbol{I}_d'(\tau = 0) = 0 \qquad \text{for } 0 \leqslant \mu \leqslant 1 \quad (18a)
$$
$$
\boldsymbol{I}_d'(\tau = \tau_0) = 0 \qquad \text{for } -1 \leqslant \mu \leqslant 0. \quad (18b)
$$

After solving equation (16) we have the diffuse modified Stokes vector in the frequency domain. We can obtain the time-domain diffuse modified Stokes vector by

$$
\boldsymbol{I}_d(t, \tau) = \frac{1}{2\pi}\int \boldsymbol{I}_d'(\omega', \tau)\exp\left(\mathrm{i}\omega\frac{\tau}{\tau_0} - \mathrm{i}\omega't\right)\mathrm{d}\omega'. \quad (19)
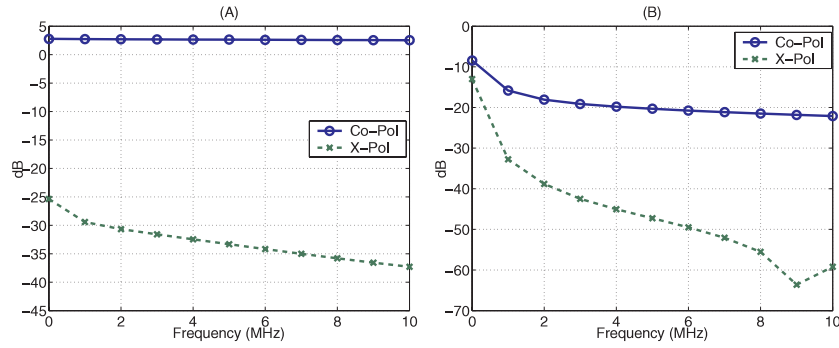$$

3. Linear and circular photon density waves through random media

To solve equation (16) we expand the specific intensity in Fourier series in the azimuthal (ϕ) domain. A detailed explanation is presented in our previous works [10, 13]. For linear polarization, the specific intensity is non-zero in mode zero and mode two, and for circular polarization, it is non-zero only in mode zero. We also integrate the Mueller matrix with respect to the azimuthal dependence expressed as

$$
\boldsymbol{L}(\mu, \mu') = \int_0^{2\pi} \boldsymbol{S}(\mu, \mu', \phi' - \phi)\,\mathrm{d}(\phi' - \phi). \quad (20)
$$

In the case of the delta function pulse, equation (16) reduces to

$$
\mu\frac{\partial}{\partial\tau}\boldsymbol{I}_d'(\omega', \tau, \mu) + \left[1 + (\mu - 1)\mathrm{i}\frac{\omega' + \omega_m}{\tau_0}\right]\boldsymbol{I}_d'(\omega, \tau, \mu) = \int_{-1}^1 \boldsymbol{L}(\mu, \mu')\boldsymbol{I}_d'(\omega', \tau, \mu')\,\mathrm{d}\mu'
$$
$$
+ \boldsymbol{F}_0(\mu)\exp(-\tau), \quad \text{for } 0 \leqslant \tau \leqslant \tau_0. \quad (21)
$$

Figure 3. Diffuse intensity of CW photon density waves as a function of the modulation frequency; (*a*) circular polarization with an optical depth of 1 and (*b*) circular polarization with an optical depth of 10.

Table 1. Particle size distribution of the fog.

	Distribution							
Diameter of particle (μm)	0.4	0.6	0.7	1.4	2.0	3.6	5.4	8.0
Number of particles	3	10	40	50	7	1	9	2

By applying the Gauss quadrature formula [12] of order N in μ dependent to equation (16), we obtain a first-order differential equation in the form

$$\frac{\partial}{\partial \tau} I + AI = B \exp(-\tau) \tag{22}$$

where

$$I = [\, I'_d(\omega', \tau, \mu_{-N}) \cdots I'_d(\omega', \tau, \mu_N) \,]^T \tag{23}$$

$$A_{j,k} = \frac{1}{\mu_j}\left[1 + (\mu_j - 1)i\frac{\omega' + \omega_m}{\tau_0} \right] - \frac{L(\mu_j, \mu_k)}{\mu_j} \tag{24}$$

$$B_{j,k} = \frac{F_0(\mu_j)}{\mu_j}. \tag{25}$$

The solution to equation (22) consists of the particular solution and the complementary solution. By imposing the boundary conditions in equations (18*a*) and (18*b*), we can find the complete solution. We separately solve equation (16) for linear and circular polarizations. In the linear polarization case, only mode zero and mode two are non-zero, and in the circular polarization case only mode zero is non-zero. We use a wavelength of 1 μm. The random medium is fog particles, assumed to be spheres of water, with size distributions shown in table 1 suspended in the air. Therefore, the Mueller matrix can be calculated based on Mie solution [16]. The path length of the medium (L) is 1 km. The concentration of fog particles is varied according to the optical depth. For linear polarization, the co-polarized component in the forward direction is in the x direction and the cross-polarized component is in the y direction. On the other hand, for circular polarization, the co-polarized component in the forward direction is left-handed and the cross-polarized component is right-handed. We investigate the following.

3.1. The effects of modulation frequency on the diffuse intensity

The transmitted continuous wave (CW) diffuse photon density intensities through the medium at $0.68°$ are shown as a function of modulation frequency in figure 3. Here, we consider cases
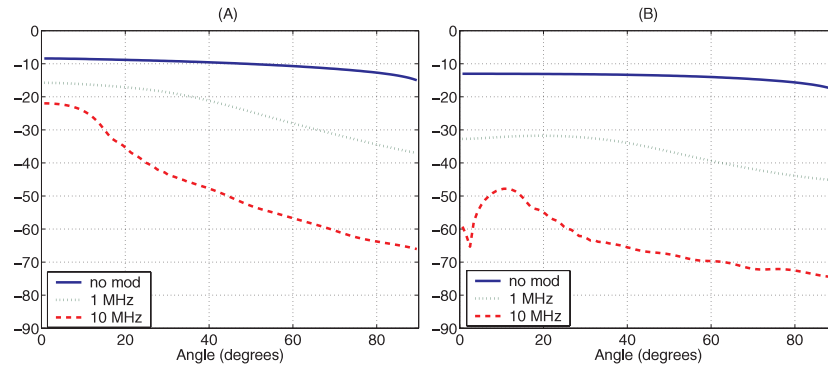
Figure 4. Angular spectrum of diffuse intensity of CW photon density waves at optical depth of 10 with different modulation frequencies; (*a*) circular co-polarization and (*b*) circular cross-polarization.
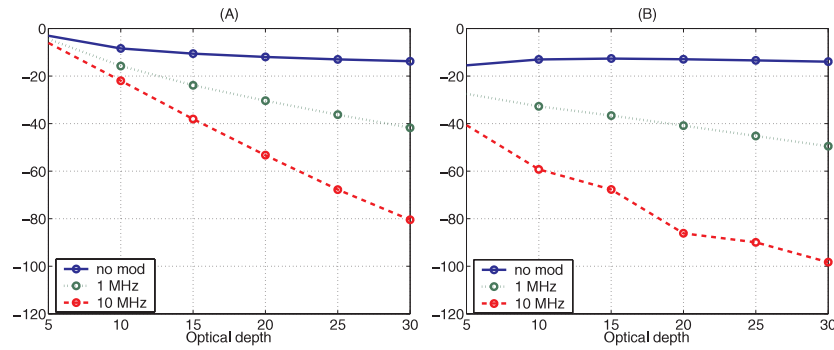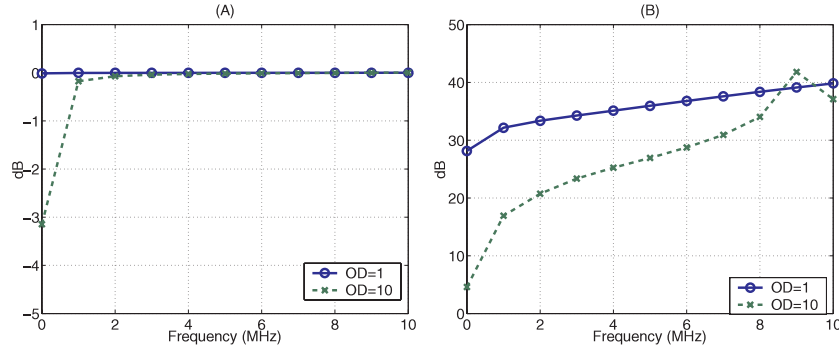

Figure 5. Diffused intensity of CW photon density waves with different modulation frequencies as a function of optical depth; (*a*) circular co-polarization and (*b*) circular cross-polarization.

of small optical depth (OD = 1) and large optical depth (OD = 10). For an optical depth of 1, the co-polarized photon density wave does not show any change as a function of the modulation frequency. However, the cross-polarization component reduces as the modulation frequency increases. On the other hand, for an optical depth of 10, the photon density wave reduces drastically as the modulation frequency increases. The reduction is more pronounced in the cross-polarized wave. This suggests that photon density waves exhibits less effect from the scattering through the random medium than regular waves. Also, the larger the modulation frequency, the smaller the effect from the scattering.

Consider the optical depth of 10 case, figure 4 shows the angular spectrum of the CW wave compared to photon density waves with modulation frequencies of 1 and 10 MHz. We notice that the angular spectrum of the photon density waves is narrower than that of a regular wave, and it is also sharper as the modulation frequency increases. This suggests that photon density waves propagate more of their energy along the optical axis compared to the regular wave.

Figure 5 compares the forward intensity (0.68°) at different modulation frequencies as a function of optical depth. For larger modulation frequencies, the co-polarized intensity reduces much more rapidly when the optical depth increases. Notice that for a regular wave, the cross-polarized wave increases and then saturates as the optical depth gets larger. Interestingly, the

Figure 6. Polarization characteristics of CW photon density waves as a function of the modulation frequency; (*a*) DOP of circular polarization and (*b*) XPD of circular polarization.

cross-polarized intensity of the photon density behaves very differently. It decreases as optical depth increases with a faster rate when the modulation frequency increases.

3.2. The effects of modulation frequency on the polarization characteristics

We consider the DOP and the XPD defined by

$$DOP(dB) = 10 \log \left[\frac{\sqrt{(I_1 - I_2)^2 + U^2 + V^2}}{I_1 + I_2} \right] \tag{26}$$

$$XPD(dB) = 10 \log \left(\frac{I_{co-pol}}{I_{x-pol}} \right). \tag{27}$$

Forward (0.68°) DOP and XPD behaviours as a function of the modulation frequency are captured in figure 6. Note that the wave at a modulation frequency of zero represents the regular wave. Here, we compare two cases of optical depth. For a small optical depth (OD = 1), both regular and photon density waves still retain their DOP and the modulation frequency does not appear to effect the DOP of the photon density wave. However, the large optical depth (OD = 10) case shows that a regular wave suffers from depolarization while the DOP of the photon density wave remains the same. Corresponding to the behaviour of intensity explained previously, the XPD of the photon density waves is larger than that of the regular wave. In addition, it improves as the modulation frequency becomes larger. The relative rate of increase for the XPD is more significant in the case of large optical depth. It infers that the photon density waves retain their energy in the original polarization better than the regular wave.

Figure 7 shows the DOP and XPD as functions of angle when the optical depth is 10. The results show that the DOP of the photon density waves remains at relatively the same level in every direction of propagation. The XPD of the photon density waves show a sharp decrease from the optical axis. This substantiates the claim we made previously that the photon density waves retain their energy in the original polarization better and do so in a much narrower angle of forward propagation.

Figure 8 shows the forward (0.68°) DOP and XPD as functions of optical depth. We notice that the photon density waves with higher modulation frequency maintain their DOP even when optical depth increases. Also, the XPD of a photon density wave is higher than that of a regular wave. This suggests that a photon density wave is less susceptible to change of its polarization state in the multiple scattering environment.
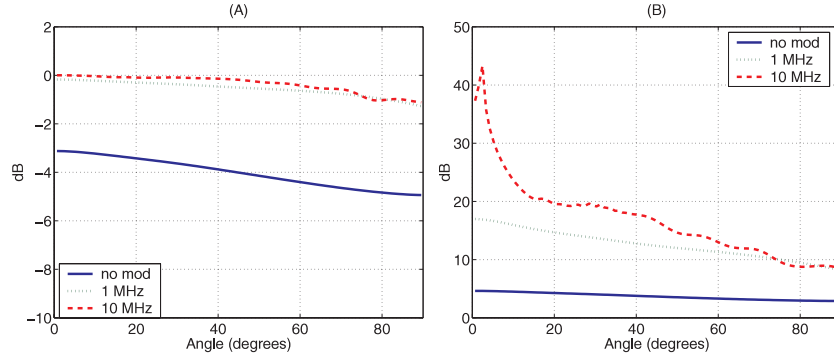
Figure 7. Polarization characteristics of photon density waves at an optical depth of 10 with different modulation frequencies as functions of angle; (*a*) DOP of circular polarization and (*b*) XPD of circular polarization.
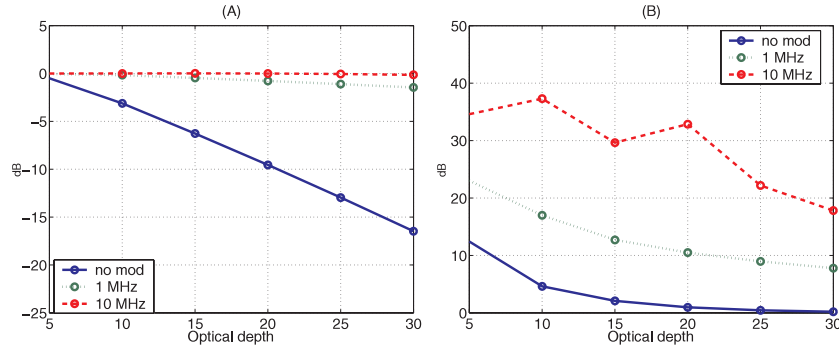

Figure 8. Polarization characteristics of photon density waves with different modulation frequencies as functions of optical depth; (*a*) DOP of circular polarization and (*b*) XPD of circular polarization.
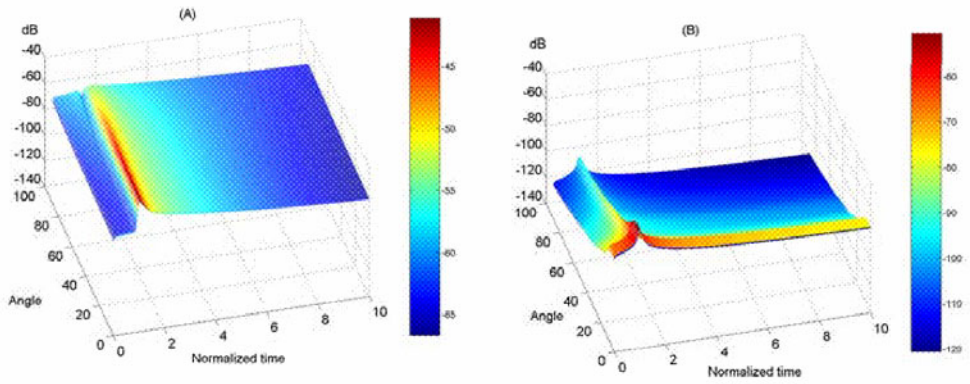
3.3. The pulse photon density waves

Pulse shapes of a circularly co-polarized wave as functions of time and angle are illustrated in figure 9. Figure 10 exhibits the same for a linearly co-polarized wave. We show the time behaviour of a pulse in the forward scattering angle ($0.68°$) in figure 11. The results show that pulse photon density wave maintains the shape of the original input pulse while the regular pulse wave shows some pulse broadening. This confirms that the photon density waves suffer less effect from the scattering. In addition, it is important to note that the level of intensity of the diffuse photon density waves is much lower than that of the regular wave.

It is also important to note that we compare our results with the diffusion approximation explained by Ishimaru [12]. In the diffusion approximation, it is assumed that the wave encounters a large number of scattering events in the medium, thus the intensity is the combination of the average intensity and very small amount of forward flux. Therefore, the angular spectrum of the intensity is very broad, and almost isotropic. Furthermore, the diffusion approximation does not provide polarization information. Thus, we can only compare the intensity behaviour, and the results of the diffusion approximation are not accurate and are overestimated in the case of large optical depths.
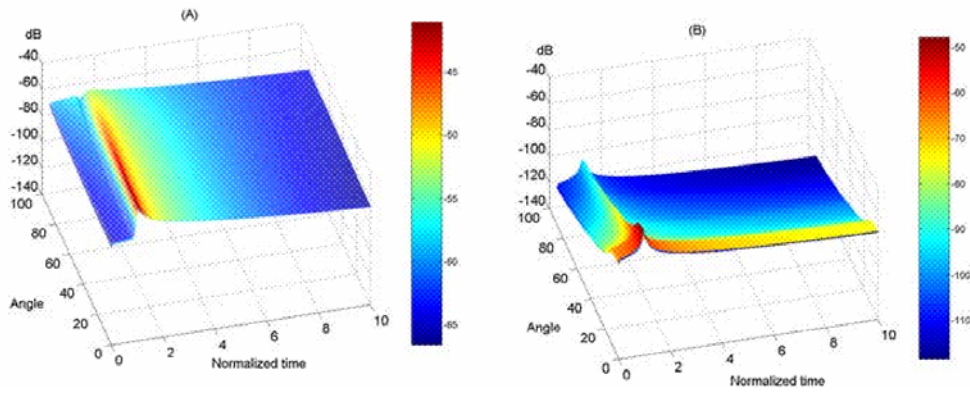
Figure 9. Circular co-polarized incoherent intensity of; (*a*) pulse waves and (*b*) pulse photon density waves with 10 MHz modulation.
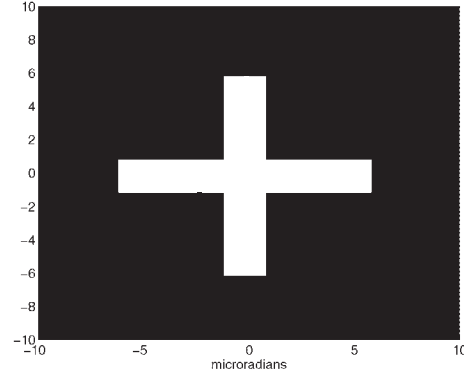

Figure 10. Linear co-polarized incoherent intensity of; (*a*) pulse waves and (*b*) pulse photon density waves with 10 MHz modulation.
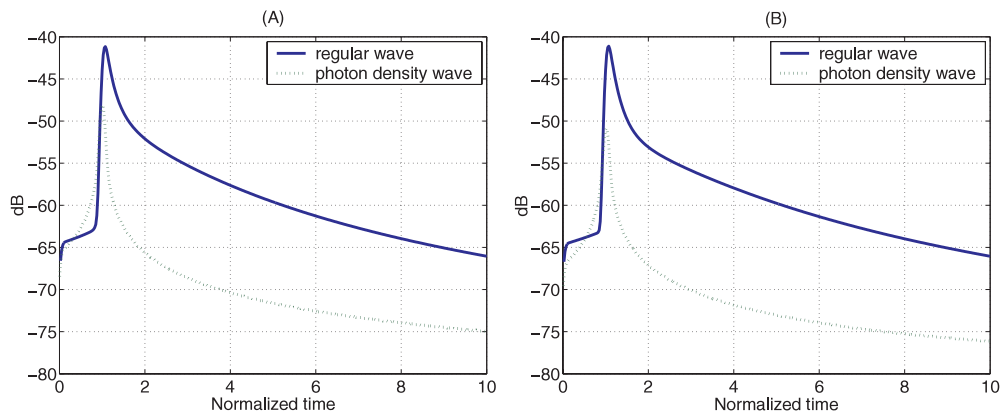
Figure 11. Forward pulse CW wave and 10 MHz photon density wave (0.68°) as a function of time; (*a*) circular polarization and (*b*) linear polarization.
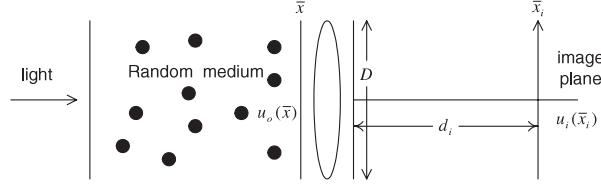
Figure 12. An imaging system.

Figure 13. A cross image.

4. Photon density waves for imaging

Different techniques are proposed to improve imaging through random media. They are based on the assumption that the scattering effect from random media creates background noise that impairs the contrast of the images. The OAIS and CPIS methods are believed to help alleviate the effect from scattering. OAIS is based on the assumption that the off-axis component of the wave comes from scattering and CPIS is based on the assumption that the cross-polarized component of the wave is the result of the scattering. On the other hand, photon density wave characteristics show that they are less influenced by the scattering of random media. Thus, using the photon density wave could produce better images.

Here, we provide an example of how photon density waves improve the contrast of images. We conduct numerical simulations using a cross image. We consider the imaging system shown in figure 12. From our previous report [14], the intensity at the imaging plane is given by

$$I_i(\bar{s}_i) = \frac{k^2}{(2\pi d_i)^2}(\pi a^2)^2 \left\{ \exp(-\tau_0) \left[\frac{J_1(ks_i a)}{(ks_i a/2)} \right]^2 + \frac{1}{\pi}\left(\frac{\lambda}{a}\right)^2 I_{inc}(\bar{s}_i) \right\} \qquad (28)$$

where J_1 is the Bessel function of the first order, a is the radius of the aperture, $s_i = \sin\theta$ and I_{inc} is the incoherent intensity calculated from the radiative transfer equation explained in the previous sections. To be able to compare with the other techniques, we define the contrast as

$$C = \frac{I_{i-coh}(s_i = 0) - I_{i-inc}(s_i = 0)}{I_{i-coh}(s_i = 0)}. \qquad (29)$$

A cross pattern shown in figure 13 is imaged through random media. The angular size of a cross extends from -10 to 10 μrad. The circular lens has a 1 m aperture size (D) and the
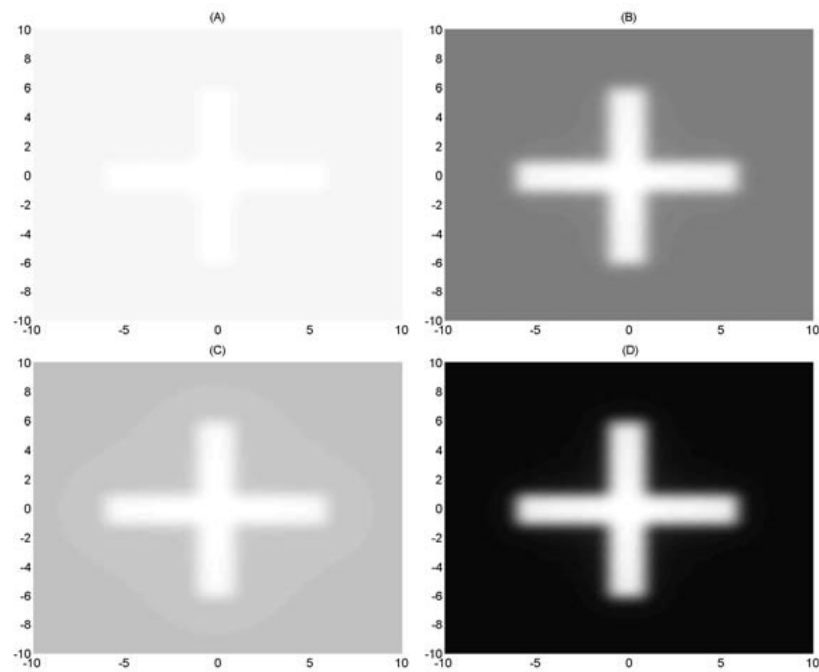
Figure 14. The circular polarized cross images through random media of optical depth 30 using; (*a*) co-polarized wave, (*b*) CPIS, (*c*) OAIS, and (*d*) 1 MHz photon density waves. The angular sizes are in microradians.

Table 2. Contrast of the cross images.

	Optical depth = 30	
	CP	LP
Co-pol	0.7429	0.7730
CPIS	38.5695	171.3048
OAIS	10.6032	10.9085
1 MHz PWD	1093.9780	1011.2420

wavelength is 1 μm. The random medium in this case is fog particles in an air background, as explained previously. The path length of the random medium is 1 km. The number density of particles is adjusted to give an optical depth of 30. The images obtained using different techniques are shown in figures 14 and 15 in the circular polarization and linear polarization cases, respectively.

Table 2 lists the contrast of these images using equation (29) in the case of optical depth 30. From the results, it appears that the photon density waves visually give better images and perform better in term of contrast, which corresponds to the calculated contrast.

Although we illustrate these examples in the scenario of atmospheric imaging applications, the same concept can be applied to the other applications, such as medical optics. In medical optics, the length of the medium is much smaller. Therefore, to achieve the same performance as the examples shown, the modulation frequency should be increased.
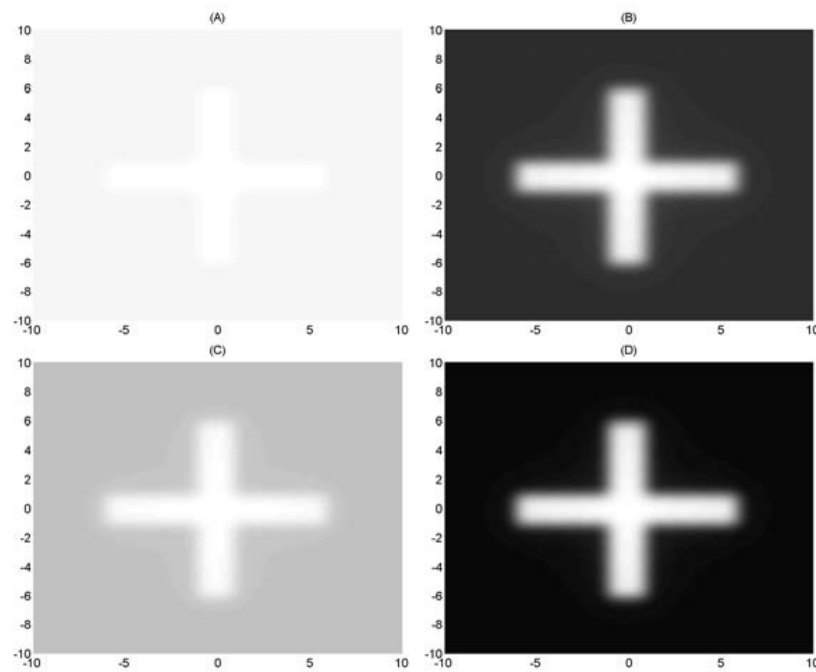
Figure 15. The linear polarized cross images through random media of optical depth 30 using; (*a*) a co-polarized wave, (*b*) CPIS, (*c*) OAIS and (*d*) 1 MHz photon density waves. The angular sizes are in microradians.

5. Conclusions

We apply the radiative transfer equation to calculate the incoherent specific intensity for a photon density wave. Polarization characteristics in terms of DOP and XPD are examined. We found that generally photon density waves have a lower level of incoherent intensity. Modulation frequency strongly affects the angular spectrum and the level of intensity. Polarization characteristics also change drastically. The XPD of a photon density wave improves tremendously compared to that of the regular wave. Also, the pulse shape of a photon density wave shows less effect from multiple scattering compared to that of a regular pulse wave. We then show the numerical simulations of a cross image through a random medium using several techniques. The results suggest that the use of the photon density wave tremendously improves the quality of the images in term of contrast.

Acknowledgments

References

[1] Tromberg B J, Svaasand L O, Tsay T-T and Haskell R C 1993 Properties of photon density waves in multiple-scattering media *Appl. Opt.* **32** 607–16

[2] Fantini S and Gratton E 2000 Fluorescence photon-density waves in optically diffusive media *Opt. Commun.* **173** 73–9

[3] Fishkin J B, Fantini S, VandeVen M J and Gratton E 1996 Gigahertz photon density waves in a turbid medium: theory and experiments *Phys. Rev.* E **53** 2307–19

[4] Matson C L and Liu H 1999 Back propagation in turbid media *J. Opt. Soc. Am.* A **16** 1254–65

[5] Matson C L and Liu H 1999 Analysis of the forward problem with diffuse photon density waves in turbid media by use of a diffraction tomography model *J. Opt. Soc. Am.* A **16** 455–66

[6] Matson C L and Liu H 2000 Resolved object imaging and localization with the use of a backpropagation algorithm *Opt. Express* **6** 168–74

[7] Matson C L 1997 A diffraction tomographic model of the forward problem using diffuse photon density waves *Opt. Express* **1** 6–11

[8] Matson C L, Clark N, McMackin L and Fender J S 1997 Three-dimensional tumor localization in thick tissue with the use of diffuse photon-density waves *Appl. Opt.* **36** 214–20

[9] Matson C L, Clark N, McMackin L and Fender J S 1996 Three-dimensional tumor localization in thick tissue using measurements in a plane *OSA Trends in Optics and Photonics on Advances in Optical Imaging and Photon Migration* vol 2 pp 179–81

[10] Ishimaru A, Jaruwatanadilok S and Kuga Y 2001 Polarized pulse waves in random discrete scatterers *Appl. Opt.* **40** 5495–502

[11] Kim A D, Jaruwatanadilok S, Ishimaru A and Kuga Y 2001 Polarized light propagation and scattering in random media *SPIE* **4257-A** at press

[12] Ishimaru A 1997 *Wave Propagation and Scattering in Random Media* (New York: IEEE)

[13] Cheung R L-T and Ishimaru A 1982 A Transmission backscattering and depolarization of waves in randomly distributed spherical particles *Appl. Opt.* **21** 3792–8

[14] Jaruwatanadilok S, Ishimaru A and Kuga Y 2002 Cross-polarization intensity subtraction technique for imaging through random scattering media *Appl. Opt.* submitted

[15] Roggemann M C and Welsh B 1996 *Imaging Through Turbulence* (Boca Raton, FL: Chemical Rubber Company)

[16] Van de Hulst H C 1957 *Light Scattering by Small Particles* (New York: Dover)